Published in final edited form as:
Mol Ther. 2008 July ; 16(7): 1267–1275. doi:10.1038/mt.2008.111.

Biodistribution of Adeno-associated Virus Type-2 in Nonhuman Primates after Convection-enhanced Delivery to Brain

Janet Cunningham[1], **Philip Pivirotto**[1], **John Bringas**[1], **Brian Suzuki**[2], **Sharmila Vijay**[2], **Laura Sanftner**[2], **Marina Kitamura**[3], **Curtis Chan**[3], and **Krystof S Bankiewicz**[1]

[1]Department of Neurosurgery, University of California, San Francisco, San Francisco, California, USA

[2]Avigen, Inc., Alameda, California, USA

[3]Preclinical Services, Charles River Laboratories, Sparks, Nevada, USA

Abstract

A combination treatment of AAV2-hAADC with oral levodopa is a novel therapeutic approach that is being developed for late-stage Parkinson's disease. Biodistribution of AAV2-hAADC was assessed over a wide range of vector dose in 12 monkeys with parkinsonian syndrome, 6 months after intraputamenal infusion. Quantitative PCR (Q-PCR) from all the major neuroanatomical regions of the brain indicated a dose-dependent increase in vector DNA, with 99% being detected in the target site and other basal ganglia tissues. Within these tissues, the distribution varied widely between the putamen (PT) and the globus pallidus, and this was attributed to differences in vector transport. Q-PCR and immunocytochemistry were consistent with results reported earlier for various measures of transgene expression including aromatic L-amino acid decarboxylase (AADC) activity assays, behavioral response, and *in vivo* imaging with positron emission tomography (PET). Outside of the brain, trace amounts of vector DNA were detected in the spleens of animals in the two highest dose groups, but not in any other peripheral tissue, blood, or cerebrospinal fluid. Some increase in neutralizing antibody titers to adeno-associated virus type-2 (AAV2) capsid protein was observed in monkeys that received high doses of AAV2-hAADC or control AAV2-GFP. This study further validates convection-enhanced delivery (CED) as the preferred method of viral vector delivery to the brain, and supports a Phase I clinical testing of AAV2-hAADC in humans with Parkinson's disease.

Introduction

The development of recombinant adeno-associated viral (AAV) vectors may provide therapeutic alternatives for neurological disorders in which conventional therapies are problematic or nonexistent. AAV type-2 (AAV2) is one of several AAV serotypes that are suitable for use in central nervous system (CNS) applications because of their tropism for neurons and ability to drive long-term expression. AAVs are derived from a nonpathogenic virus, and numerous *in vivo* studies have shown that they are safe to use and typically elicit no cytotoxic effects and relatively minor immune response. The long-term therapeutic effect of AAV vectors that has been observed in animal models, however, has not always translated to clinical studies in humans. Hemophilia patients treated with AAV2-factor IX experienced a decline in transgene expression and transient elevation of liver transaminases within 8 weeks after vector infusion into the hepatic artery.[1] It is now believed that cell-mediated immunity-

Correspondence: Krystof S. Bankiewicz, University of California, San Francisco, 1855 Folsom Street, Room 230, San Francisco, California 94103-0555, USA. krystof.bankiewicz@ucsf.edu.

targeting antigen of the AAV capsid resulted in destruction of the transduced hepatocytes, and that immunosuppressive regimens may be effective in preventing this response.[2] Alternatively, AAV therapies that employ different delivery routes and lower vector doses may encounter fewer immunological challenges. Given the lack of an adaptive immune response in brain parenchyma, and its separation from the general circulation by the blood–brain barrier, intraparenchymal injections of AAV vectors may prove to be less problematic in this regard.[3] Preclinical studies have shown, however, that very high titers of AAV can induce a transient innate inflammatory response when infused into striatum.[4]

In little more than a decade, preclinical studies of AAV in the CNS have progressed from simple injections into rodent brains with reporter gene vectors to refined delivery of a vast array of potential therapeutics in rodent and primate models of disease. A small number of these potential therapies have advanced to phase I clinical testing, including intraputamenal convection-enhanced delivery (CED) of AAV2-hAADC for treatment of advanced Parkinson's disease (PD).[5–8] AAV2-hAADC expresses human aromatic L-amino acid decarboxylase (AADC) which constitutes the last enzymatic step in the biosynthesis of dopamine. Safety and efficacy data for AAV2-hAADC have been published,[9–14] including two nonhuman primate studies focused on clinical response and transgene expression over the long term (>6 years)[15] or for 6 months over a wide range of vector dose.[16] In addition, the dose-ranging study was designed to include an extensive assessment of vector biodistribution, and is the focus of this report. Biodistribution is factored into the regulatory approval process for gene therapy clinical studies because it constitutes an important safety issue. Inadvertent distribution of viral capsid proteins and transgenes to nontargeted tissues could potentially have deleterious effects such as exacerbation of immune response, undesirable biochemical changes associated with transgene expression in nonnative tissue, and germline transmission of vector DNA. However, other than a benign humoral response to the AAV2 capsid, such effects were not found in this analysis. The data from this study provide an in-depth and comprehensive description of AAV2 vector trafficking in brain and peripheral tissues after intraputamenal delivery, and illustrate how such trafficking is related to dose.

Results

We have earlier reported results from a dose-ranging study of AAV2-hAADC therapy in nonhuman primates with parkinsonian syndrome.[16] In that study, twelve MPTP (1-methyl-4-phenyl-1,2,3,6-tetrahydropyridine)-HCl-lesioned rhesus macaques were infused with AAV2-hAADC by CED for assessing biodistribution, transgene expression, and behavioral response. Magnetic resonance imaging was employed to identify stereotactic coordinates for the postcommissural putamen (PT) (most affected region of the striatum) in each subject. Ten animals in five dose groups received bilateral intraputamenal infusions (2/hemisphere; 4/brain) of AAV2-hAADC at doses of 6, 18, 55, 170, and 500 U/hemisphere or, in terms of total dose, 12, 36, 110, 340, and 1,000 U/brain. (Note: 1 U = 1×10^9 vector genomes (vg) of AAV2.) Two control animals were similarly infused with AAV2-GFP at doses of 1,000 U/brain. Prior to the gene transfer and during the 6 months after the transfer, animals were assessed for transgene expression using *in vivo* positron emission tomography (PET) which measures striatal uptake of the AADC tracer 6-[^{18}F]fluoro-L-*m*-tyrosine. Clinical response was evaluated in terms of a Parkinson's disease (PD) clinical rating scale, both in the absence and presence of L-dopa treatment. As reported earlier, dramatic improvements in behavioral response were observed above a threshold of ~55 U/hemisphere, coupled with robust restoration of AADC activity, as evidenced by PET.[16] After completing the in-life phase of the study we studied biodistribution using PCR and immunohistochemistry (IHC), which is the focus of this report. Changes in AAV2-neutralizing antibody titers are also presented here.

Biodistribution (PCR analyses)

Six months after vector infusion, quantitative PCR (Q-PCR) was performed to measure levels of vector DNA in serum, CSF, heart, liver, lung, kidney, spleen, thymus, salivary gland, gonadal tissue, and in 13 neuroanatomical regions from one side of the brain (ipsilateral to MPTP infusion). Relative to vector dose, high levels of hAADC complementary DNA (cDNA) (up to 1,218,084 copies/μg genomic DNA) were detected at the infusion site (PT) of almost every animal treated with AAV2-hAADC (Table 1). The levels were approximately dose-dependent, although large discrepancies were noted within the two groups that had received the highest doses. The reasons for these differences could include sampling error or problems with vector delivery (especially with respect to PT in RQ3715 where only trace amounts of hAADC were found). Alternatively, (as recent evidence suggests), variability in vector transport away from the target area through perivascular mechanisms may also play a role.[17, 18] Outside of the injection site, significant levels of vector DNA (up to 279,187 copies/μg genomic DNA) were also detected in the globus pallidus (GP, including GPi and GPe) from almost all the treated animals. In regard to this finding, it is highly unlikely that the vector was accidentally infused into the GP. Given that individual magnetic resonance images were used for guiding each stereotactic delivery, very high accuracy was achieved in terms of targeting the PT. Brain hemispheres that were dissected and processed for PCR could not be evaluated histologically; however, such an analysis of the contralateral hemispheres in all the animals revealed that needle tracks were placed correctly in the PT and not in the GP even though transgene expression was consistently observed in both tissues (representative tissue sections are shown in Supplementary Figures S1–S3). Next, very low levels of hAADC cDNA were detected in other sampled regions of the brains of animals that had received 500 U AAV2, suggesting very limited dispersion of the vector from the infusion site in this high-dose group. A similar distribution was seen in the second- and third-highest groups, but not as widespread. Indeed, it was quite striking to note that the vector remained so closely confined to the striatum (PT and caudate nucleus; CN) and the GP in all the dose groups. Table 1 also illustrates that in 7 of the 10 AAV2-hAADC-treated animals, 99% (RQ3714, RQ3723, and RQ3672) or 100% (RQ3719, RQ3840, RQ3811, and RQ3753) of the PCR signal was generated from these basal ganglia tissues. Two of the ten animals, RQ3702 and RQ3746, had 98 and 96% of their vector DNA, respectively, in these tissues. The average amount of signal generated from PT, CN, and GP for these animals (9 of the 10 monkeys treated with AAV2-hAADC) was 99%. As mentioned earlier, RQ3715 appears to be an outlier, showing high percentages of vector distributed in tissues distant from the PT and GP. However, the actual copy numbers in these tissues were very low (similar to those seen in adjacent dose groups), thereby suggesting that the percentage data for this animal represent an artifact of problematic delivery or sampling error at the infusion site. PCR efficiency was also assessed. The overall efficiency of the PCR reaction was 93–95%, as determined from the slopes of the PCR standard curves. The efficiency of the PCR reaction varied in individual brain tissues ($n = 148$) that were spiked with known amounts of target DNA, probably because of the presence of inhibitors. Reactions that were <75% efficient ($n = 15$) were considered to have suboptimal sensitivity and are flagged in Table 1. PCR efficiency for these 15 brain tissues ranged from 14 to 74%, with a median of 60%.

Outside of the brain, trace amounts of vector DNA (50–218 copies/μg genomic DNA) were detected in spleen samples from animals in the two highest dose groups, but not in any other peripheral tissue, serum, or cerebrospinal fluid (Supplementary Table S1). It is important to note that PCR efficiency in spiked samples was low (<75%) in most of the serum and CSF, because of the acellular nature of the samples and perhaps also because of the presence of inhibitors; therefore the possibility of false negatives cannot be ruled out. Of the 47 serum and CSF samples tested, 41 exhibited <75% efficiency (ranging from 0 to 73% with a median of 28%). The PCR efficiency of spiked samples was high for most of the other peripheral tissues, with the exception of some of the lung samples (Supplementary Table S1). In addition, all brain

tissue, peripheral tissue, serum samples, and CSF samples from AAV2-GFP-treated control animals were free of detectable vector sequence (Table 1 and Supplementary Table S1).

AADC transgene expression (IHC)

The density of AADC-positive cells in the targeted PT region was determined by immunostaining fixed sections of brain tissue from the side contralateral to MPTP treatment with a primary antibody to human AADC and immunoperoxidase-labeled secondary antibody. Manual cell counts were performed under ×100 original magnification with a counting grid at six randomly selected sites in each section. Regression analysis demonstrated a dose-dependent increase in density of AADC-stained cells (Figure 1). Both the control group and the lowest-dose group showed nil or very little coverage of the PT by AADC-positive cells, the middle three groups showed intermediate levels of staining comparable to one another, and the highest-dose group was well covered, with visibly higher numbers of positive cells.

Measurement of the areas of AADC expression in the same stained tissue sections suggested slightly different results. Very few AADC-positive neurons were found in the control and lowest-dose groups, as expected, but the areas of coverage were very similar among the other four AAV2-hAADC groups (Figure 2). This suggests that the distance of vector spread is the same regardless of dose, and the increased transgene expression in higher dose groups can be attributed to higher concentrations of transduced cells within that covered distance. Immunoperoxidase-labeled sections representative of those used for cell counts are shown in Figure 3c and d.

Tissue sections stained for IHC analysis were also examined under low magnification to illustrate dose-dependent hAADC expression (Figure 3a and b). While background staining does not appear to be an issue in this study (note especially the control animals and the lowest AAV2-hAADC dose group), it cannot be completely ruled out as a contributor to the appearance of high expression observed in some groups. There is a low amount of crossreactivity between the primary antibody and monkey endogenous AADC. While MPTP lesioning virtually eliminates this issue because it destroys nigral (dopaminergic) neurons that extend axonal processes to the striatum, lesioning is never as complete on the side contralateral to MPTP treatment. Under high magnification, however, potential endogenous AADC staining (located in residual dopaminergic fibers) would be easily distinguished from expression of the transgene (located in neuronal cell bodies) (Figure 3c and d). In the context of these considerations, the low magnification (×20) images in Figure 3a and b provide further evidence that CED is a highly effective method of spreading the vector throughout the entire targeted striatal area.

Neutralizing antibody response

One of the criteria for including an animal in this study was absent or low neutralizing antibody titer to AAV2 capsid protein (<1:100). Actual preinfusion titers ranged from <1:10 to <1:50. Six months after AAV2-hAADC or AAV2-GFP treatment, antibody titers in all the animals were measured again. Three animals developed titers up to 100-fold over baseline, including one monkey each from the two highest-dose treatment groups (170 and 500 U AAV2-hAADC) and one from the control group (500 U AAV2-GFP) (Table 2). A majority of the animals showed some increase over baseline, with the exception of RQ3715, RQ3723, and RQ3753. Antibody response can be highly variable between animals within the same group, depending on how much systemic exposure occurs during delivery. However, because RQ3715 was in one of the highest-dose groups (170 U/hemisphere), the observed lack of antibody response is interpreted as further evidence of a delivery problem in this animal. Given that four infusion cannulae are used for each brain, it is possible that the error occurred on the ipsilateral side only, as suggested by PCR data, and not in contralateral tissue used for cytochemical analyses.

Discussion

Biodistribution of AAV2-hAADC in brain and peripheral tissues has been assessed in five dose groups and one control group of monkeys with parkinsonian syndrome 6 months after intraputamenal infusion. Total copies of vector DNA increased in the brain in a roughly dose-dependent manner. The results were highly consistent with transgene expression as measured by high-performance liquid chromatography analysis of AADC enzymatic activity (performed on adjacent tissue punches; reported previously),[16] and mostly consistent with expression as measured by IHC (performed on the contralateral hemisphere; reported here), behavioral response,[16] and *in vivo* PET imaging of 6-[^{18}F]fluoro-L-*m*-tyrosine uptake.[16] PCR analyses of samples collected from every major neuroanatomical region showed that an average of 99% of vector stayed confined to basal ganglia tissues—mostly PT and GP, and to a limited extent, CN. (RQ3715 is excluded from this calculation as being an outlier, as explained in Results.) The relative amounts of vector DNA in PT versus GP varied widely among the animals, ranging from 35 to 99% in PT and 0 to 65% in GP. Indeed, even within dose groups, vector distribution varied widely between these two regional tissues. For instance, in the lowest-dose group, the ratio of PT to GP distribution in RQ3753 was 35 to 65%, whereas in RQ3811 it was 96 to 4%. Similar differences were observed in the highest and middle groups. These observations confirm earlier results in rodents and monkeys that showed vector expression in both PT and GP after intrastriatal delivery of AAV.[11,13,19] In human PD patients, transport of AAV2-hAADC to the GP would not be expected to be problematic. Although the striatum is by far the major target of midbrain dopaminergic projections from the substantia nigra pars compacta, the GP also receives significant dopaminergic input from the substantia nigra pars compacta.[20,21] Unlike nigrostriatal neurons, the nigropallidal pathway is relatively spared in PD, and provides a compensatory mechanism for dopamine replacement, at least in the early stages of the disease.[22–25] Because the nature of this mechanism is not understood, however, it is not known whether production of dopamine by AAV2-hAADC in the GP would have a similar compensatory effect. On the other hand, the potential for therapeutic effect from vector distributed to CN is more apparent. Like PT, the CN facilitates dopamine signaling under normal conditions and becomes profoundly dopamine-deficient in PD.[26] In addition, long-term safety and efficacy data have been demonstrated in monkeys with parkinsonian syndrome that received CED of AAV2-hAADC into both PT and CN.[15]

AAV2-hAADC's biodistribution profile supports its intended use in PD therapy, given that dopamine functions as an essential neurotransmitter, at some level, throughout all basal ganglia structures, and is sharply decreased in the disease. Even so, an understanding of the mechanisms through which viral vectors become dispersed throughout the CNS will be essential for developing and optimizing neurological molecular therapies. Transgene expression that can be detected at substantial distances from the injection site has been interpreted as evidence of neuronal transport with respect to a number of viral vectors.[27,28] Recent studies have shown, however, that CED achieves broad distribution of viral particles by working in concert with the brain's natural propensity to pump fluids and molecules along perivascular spaces.[17,18,29] The concept of the “perivascular pump,” a means of propelling molecules within the CNS along the outside of the vasculature by cardiac pulsations, has been validated in several studies, and predates the field of gene therapy.[30,31] Hadaczek *et al.* demonstrated the relevance of this concept to CED of AAV2 by comparing volumes of vector distribution in brains of rats whose heart rates and blood pressure were modulated. In rats with high blood flow, AAV2 was found in 4.4-fold and 16.5-fold greater volume of striatal tissue as compared to groups with low or no blood flow, respectively.[17] Furthermore, trafficking to GP was observed only in the high-blood-flow group, which is consistent with the theory that perivascular transport is responsible for the biodistribution pattern observed in this nonhuman primate study. PT and GP are physically adjacent in the primate brain, and both are vascularized by lenticulostriate branches of the middle cerebral artery.[32] While a small body of clinical evidence suggests that PT and

GP at least partly share this vasculature,[33] an imaging study in which 30 brains were injected with gelatinous Indian ink concluded that these tissues have vascular networks that are proximal to one another, but separate.[34] While further studies are needed to determine the relevance of the rodent data to the nonhuman primate results reported here, it is possible that both neuronal transport and perivascular mechanisms significantly influence biodistribution of AAV2 in the brain after intraputamenal infusion. Variable delivery also influences biodistribution, and is not uncommon in brain infusion procedures. Leakage of infusate from targeted sites such as PT into surrounding sulci and ventricles can occur during CED and almost certainly negatively impacts therapeutic effect, although recent advances in real-time brain imaging show promise in addressing this issue.[35] Such leakage may also result in uptake of AAV particles by dendritic cells lining the ventricles, migration of these cells to deep cervical lymph nodes that drain the brain and CSF, and stimulation of T-cell and B-cell responses to AAV capsid protein.[3] However, other than a benign rise in antibody titers, no untoward effects related to immune response have been reported in the limited number of CNS clinical studies that have employed AAV vectors.[5–8] Finally, serotype also influences AAV transduction (both "spread" and tissue tropism) in the brain. AAV1 and AAV5 transduce larger volumes of brain tissue in rats as compared to AAV2, and exhibit greater capacities for retrograde transport.[36,37] Many other human-derived and nonhuman primate-derived serotypes show similar promise in both mice and rats,[38,39] and some reveal different patterns of transduction in a diverse array of CNS tissues.[40] While most serotype comparisons have been done in rodents, meaningful long-term expression data and confirmation of tissue tropisms will need to be obtained in nonhuman primates, in which the size and neuroanatomy of the brain, transcriptional (and/or other cellular) mechanisms, and the lifespan of the animal more closely resemble those of humans.

Biodistribution was also assessed in eight peripheral organs, in the serum, and in the CSF to determine whether AAV2-hAADC delivered to the brain can spread to nonneurological tissues. No vector DNA was detected in fluids or tissues, other than trace amounts in spleen in the two highest-dose groups. These results suggest that there was limited systemic exposure to vector, or that disseminated vector was cleared before the time-point of analysis. Neutralizing antibody titers rose significantly in animals that received 170 or 500 U AAV2/hemisphere, confirming some systemic exposure at the time of delivery. The issue of neutralizing antibody response is an essential consideration in the design of clinical gene transfer studies, and has important implications for patient inclusion criteria and protocols involving readministration of the therapeutic agent. A significant portion of the human population has antibodies to wild-type AAV2, and it is not known what levels would negatively impact AAV2-hAADC therapy.[41–43] Studies have shown that AAV2 can transduce brain tissue in animals with pre-existing immunity; however, high titers of antibodies are associated with significant loss of efficiency.[12,44] Prescreening patients for low levels of neutralizing antibodies is therefore necessary in order to ensure safety and uncompromised therapeutic effect.

The biodistribution study presented here demonstrates that AAV2-hAADC delivered to PT with CED was detected in the target tissue in a roughly dose-dependent manner in a nonhuman primate model of PD. An average of 99% of infused vector stayed in basal ganglia tissues and, within these tissues, the distribution varied widely between PT and GP. This effect is consistent with previous studies in rodents and monkeys and may be because of differences between individual animals in perivascular or neuronal transport. Negligible copies of vector DNA were detected in tissues outside of the CNS, and some increases in antibody titer to AAV2 capsid were observed in very-high-vector-dose groups. This study further validates CED as a preferred method of viral vector delivery in brain, and supports a Phase I clinical testing of AAV2-hAADC in PD.

Materials and Methods

Nonhuman primate model for PD and biodistribution of AAV2

Experiments were performed in accordance with National Institutes of Health guidelines and the protocols approved by the University of California, San Francisco Institutional Animal Care and Use Committee. Twelve young (3–5 kg) rhesus macaques were prescreened for low (<1:100) pre-existing neutralizing antibody titers to AAV2. The monkeys were lesioned with MPTP-HCL through the right internal carotid artery along with follow-up intravenous administrations until a stable hemiparkinsonian syndrome was achieved, as described earlier.[16] This model mimics the biochemical, histopathological, and behavioral changes seen in advanced stages of idiopathic PD in humans. CED was employed to administer AAV2-hAADC or AAV2-GFP to stably lesioned animals (as described in the later text). Behavioral testing and PET scans were performed during the 5 months prior to gene transfer and for 6 months after vector infusion.[16] Tissue samples collected during necropsy from the side of the brain ipsilateral to MPTP lesioning (right side) were analyzed using PCR for quantifying hAADC DNA or HPLC for the purpose of measuring AADC enzyme activity. Tissue sections from the side of the brain contralateral to the MPTP infusions were subjected to immunohistochemical analysis for transgene expression.

AAV2 vectors

The human AADC cDNA was cloned into an AAV2 shuttle plasmid, and a recombinant AAV2 containing hAADC under the control of the cytomegalovirus promoter was generated by a triple transfection technique and subsequent purification by CsCl gradient centrifugation.[45, 46] AAV2-hAADC (earlier termed "AAV-hAADC" and renamed so as to clarify the serotype) was concentrated to ~4×10^{12} vg/ml as determined by Q-PCR. In the text we define 1×10^{9} vg as 1.0 U AAV2 so as to facilitate dose comparisons. Thus interconversion of vector genomes and units AAV2 is easily accomplished by inserting or removing the term "$\times 10^{9}$" after the quoted number of Units of AAV2.

Convection-enhanced delivery of AAV2

Animals were prepped for surgery as described earlier.[15] AAV2-hAADC or control AAV2-GFP was stereotactically infused bilaterally at four sites (2/hemisphere) into postcommissural PT at the following rates: 0.1 μl/min (10 minutes), 0.2 μl/min (10 minutes), 0.5 μl/min (10 minutes), 0.8 μl/min (10 minutes), and 1.0 μl/min (36 minutes). The doses of AAV2-hAADC vector used for each pair of animals were 0, 6, 18, 55, 170, or 500 U AAV2-hAADC/hemisphere, and were diluted from the concentrate (4,000 U AAV2/ml) such that each indicated dose was delivered in a volume of ~50 μl at each infusion site. The pair of animals that received no AAV2-hAADC received AAV2-GFP at 500 U/hemisphere instead. Although the animals were lesioned more heavily in the hemisphere ipsilateral to MPTP administration, the vector was delivered to both hemispheres to mimic the intended human clinical study to the extent possible, and also to provide tissue in the contralateral hemisphere for histological analysis. Approximately 10 minutes after infusion, the cannulae were raised at the rate of 1 mm/min until they were clear of both the striatum and overlying cortex. The animals were monitored for full recovery, and their behavioral characteristics were observed twice per day over the next 7 days.

PCR analyses

Isolation of DNA from serum and CSF—Serum and CSF samples were collected before administering the vector dose (day 1) and immediately prior to necropsy, and stored at approximately −70 °C. Genomic DNA was isolated from serum and CSF samples using a

genomic DNA isolation kit (Qiagen QIAamp Mini Spin Kit). A sentinel control sample was also isolated at the same time as the serum and CSF samples so as to monitor for contamination.

DNA isolation from snap frozen tissues—Samples of heart, liver, salivary gland, lung, kidney, spleen, thymus, ovaries or testes, and 13 regions of the brain were freshly frozen in dry-ice-cooled isopentane and stored at approximately −70 °C until being transferred to the PCR lab for analysis. Genomic DNA was isolated from tissue samples using a genomic DNA isolation kit (QIAamp Mini Spin Kit; Qiagen, Valencia, CA). A sentinel control sample was also isolated at the same time to monitor for contamination. The amount of total DNA isolated from each sample was determined by spectrophotometry at 260 and 280 nm wavelengths on a Molecular Devices SPECTRAMax 190 Microplate Reader.

Primer and probe design—The AAV2-hAADC vector used in this study contains human AADC cDNA. The Q-PCR primers and probe anneal to a 121-base pair region of exons 2 and 3 of the AADC gene (nt 219-339; HGNC:2719), thus spanning an intron that is not present in the vector sequence and thereby minimizing amplification of genomic DNA (forward primer: 5′-AGA CAC GTT TGA GGA CAT CA-3′; reverse primer: 5′-AAG CAT GGC CGG GTA CG-3′; TaqMan probe: 5′-6FAM-TGA CGC ACT GGC ACA GCC CCT ACT-TAMRA-3′; Applied Biosystems, Foster City, CA). The specificity of the primer/probe set was confirmed by running the reaction product on an agarose gel and detecting the predicted amplicon of the appropriate size.

Q-PCR analysis of AAV2-hAADC distribution—Q-PCR analysis of AAV2-hAADC using a fluorogenic 5′-nuclease assay was performed on an Applied Biosystems 7900HT Sequence Detection System. Real-time Q-PCR was standardized with plasmid DNA containing the vector insert. The plasmid was linearized with a restriction enzyme, purified, quantified by ultra violet absorbance, and diluted in Q-PCR dilution buffer to result in seven standards ranging from 10 to 1×10^6 copies/reaction. Each standard was run in three replicate 25 μl reactions in a 384-well optical plate. When possible, a total of 3 μg of genomic DNA from each sample was assayed for AAV2-hAADC. Of the 3-μg total, 2 μg (eight reactions containing 250 ng/reaction) were assayed for AAV2-hAADC, and the remaining 1 μg (four reactions, 250 ng/reaction) was spiked with 100 copies/μg (25 copies/reaction) of the AAV2-hAADC standard and assayed to monitor the reaction efficiency in each sample. Samples with low reaction efficiency (<75%) were presumed to contain PCR inhibitors that affected sensitivity. In the presence of AAV2-hAADC DNA, the AAV2-hAADC-specific primers amplify a 121-base pair region of the AAV2-hAADC target. During the 60 °C extension step, the AAV2-hAADC-specific probe is incorporated into the amplicon and releases the attached 6-carboxyfluorescein. The amount of fluorescence generated is proportional to the number of AAV2-hAADC amplicons generated during the run, and is related to the initial amount of AAV2-hAADC template present in each sample. Human AADC cDNA copies were calculated by multiplying the copies per well by 2, assuming that one copy of double-stranded plasmid DNA is equivalent to two single-stranded vector genomes.

Upper and lower limits of quantitation—The upper and lower limits of quantitation were selected as the highest and lowest points on the standard curve (1×10^6 copies of AAV2-hAADC/reaction and 10 copies of AAV2-hAADC/reaction, respectively).

Immunohistochemistry

Sectioning of brain tissue was performed as described earlier.[15] IHC was carried out on free-floating 40-μm coronal sections with a primary antibody specific for AADC (Chemicon, Temecula, CA; 1:1,500). Sections from around the injection site and throughout the target tissue were incubated in 3% hydrogen peroxide for 30 minutes to quench endogenous

peroxidases. After blocking nonspecific binding with 10% normal goat serum, the sections were incubated in primary antibody overnight at room temperature and then with a biotinylated anti-rabbit immunoglobulin G antibody (Vector Laboratories, Burlingame, CA; 1:300) with streptavidin-conjugated horseradish peroxidase (Vector Laboratories, 1:300) at room temperature, both for 1 hour. The complex was visualized with 3-3′-diaminobenzidine (Vector Laboratories) and hydrogen peroxide. The sections were mounted on Superfrost Plus slides (Brain Research Laboratories, Newton, MA), dried, dehydrated in ascending ethanol series, cleared in xylene, and mounted with Cytoseal-XYL (Richard-Allen Scientific, Kalamazoo, MI). The area in which hAADC-positive cells were present was calculated using National Institutes of Health Image software. Density (average number of hAADC-positive cells per site) was determined using a counting grid at six randomly selected sites in each section, and six sections (on an average) were analyzed for each animal. Care was taken to avoid quantitation bias by counting only every tenth tissue section and by selecting individual counting sites on the basis of physical parameters (such as proximity to infusion tracts and even spacing throughout tissue blocks) rather than on the presence and/or intensity of staining.

Neutralizing antibody assay

The neutralizing antibody titer of serum or plasma was determined *in vitro* in a cell-based assay. A defined number of AAV2 vector particles encoding a β-galactosidase reporter gene (AAV2-LacZ) were incubated with test serum for 1 hour at 37 °C, and the mixture was then added to HEK-293 cells near confluence in 96-well plates. The 100% level of AAV2 transduction was represented by the amount of β-galactosidase activity measured in culture 24 h after transduction with AAV2-LacZ in the presence of naive mouse serum. Half-log serial dilutions of the test serum in naive mouse serum were carried out to determine the highest serum dilution that resulted in 50% or greater inhibition of β-galactosidase expression. Each dilution series was tested in triplicate. A reference plasma with a well-defined AAV2-neutralizing titer was run in each assay, and a negative control (naive mouse serum only) was used to set the assay background. The result was typically reported as the two dilutions that bracket the 50% inhibition level, *e.g.*, 1:100–1:316.

Supplementary Material

Refer to Web version on PubMed Central for supplementary material.

Acknowledgments

We thank Avigen for providing AAV2 vector. We thank Fraser Wright for vector development and Jurg Sommer for advice on the neutralizing antibody assay. Funding for this work was provided by the National Institute of Neurological Disorders and Stroke (NINDS) Intramural Research Program, a U54 grant from NINDS, and from Avigen, Inc. (Alameda, CA) to K.S.B.

References

1. Manno CS, Pierce GF, Arruda VR, Glader B, Ragni M, Rasko JJ, et al. Successful transduction of liver in hemophilia by AAV-Factor IX and limitations imposed by the host immune response. Nat Med 2006;12:342–347. [PubMed: 16474400]
2. Jiang H, Couto LB, Patarroyo-White S, Liu T, Nagy D, Vargas JA, et al. Effects of transient immunosuppression on adenoassociated, virus-mediated, liver-directed gene transfer in rhesus macaques and implications for human gene therapy. Blood 2006;108:3321–3328. [PubMed: 16868252]
3. Lowenstein PR, Mandel RJ, Xiong WD, Kroeger K, Castro MG. Immune responses to adenovirus and adeno-associated vectors used for gene therapy of brain diseases: the role of immunological synapses in understanding the cell biology of neuroimmune interactions. Curr Gene Ther 2007;7:347–360. [PubMed: 17979681]

4. Reimsnider S, Manfredsson FP, Muzyczka N, Mandel RJ. Time course of transgene expression after intrastriatal pseudotyped rAAV2/1, rAAV2/2, rAAV2/5, and rAAV2/8 transduction in the rat. Mol Ther 2007;15:1504–1511. [PubMed: 17565350]
5. Fiandaca M, Forsayeth J, Bankiewicz K. Current status of gene therapy trials for Parkinson's disease. Exp Neurol 2007;209:51–57. [PubMed: 17920059]
6. Kaplitt MG, Feigin A, Tang C, Fitzsimons HL, Mattis P, Lawlor PA, et al. Safety and tolerability of gene therapy with an adeno-associated virus (AAV) borne GAD gene for Parkinson's disease: an open label, phase I trial. Lancet 2007;369:2097–2105. [PubMed: 17586305]
7. McPhee SW, Janson CG, Li C, Samulski RJ, Camp AS, Francis J, et al. Immune responses to AAV in a phase I study for Canavan disease. J Gene Med 2006;8:577–588. [PubMed: 16532510]
8. Eberling JL, Jagust WJ, Christine CW, Starr PA, Larson PS, Bankiewicz KS, et al. Results from a phase I safety trial of hAADC gene therapy for parkinson's disease. Neurology 2008;70:1980–1983. [PubMed: 18401019]
9. Sanftner LM, Rivera VM, Suzuki BM, Feng L, Berk L, Zhou S, et al. Dimerizer regulation of AADC expression and behavioral response in AAV-transduced 6-OHDA lesioned rats. Mol Ther 2006;13:167–174. [PubMed: 16126007]
10. Bankiewicz KS, Daadi M, Pivirotto P, Bringas J, Sanftner L, Cunningham J, et al. Focal striatal dopamine may potentiate dyskinesias in parkinsonian monkeys. Exp Neurol 2006;197:363–372. [PubMed: 16337943]
11. Hadaczek P, Kohutnicka M, Krauze MT, Bringas J, Pivirotto P, Cunningham J, et al. Convection-enhanced delivery of adeno-associated virus type 2 (AAV2) into the striatum and transport of AAV2 within monkey brain. Hum Gene Ther 2006;17:291–302. [PubMed: 16544978]
12. Sanftner LM, Suzuki BM, Doroudchi MM, Feng L, McClelland A, Forsayeth JR, et al. Striatal delivery of rAAV-hAADC to rats with preexisting immunity to AAV. Mol Ther 2004;9:403–409. [PubMed: 15006607]
13. Bankiewicz KS, Eberling JL, Kohutnicka M, Jagust W, Pivirotto P, Bringas J, et al. Convection-enhanced delivery of AAV vector in parkinsonian monkeys; *in vivo* detection of gene expression and restoration of dopaminergic function using pro-drug approach. Exp Neurol 2000;164:2–14. [PubMed: 10877910]
14. Sanchez-Pernaute R, Harvey-White J, Cunningham J, Bankiewicz KS. Functional effect of adeno-associated virus mediated gene transfer of aromatic L-amino acid decarboxylase into the striatum of 6-OHDA-lesioned rats. Mol Ther 2001;4:324–330. [PubMed: 11592835]
15. Bankiewicz KS, Forsayeth J, Eberling JL, Sanchez-Pernaute R, Pivirotto P, Bringas J, et al. Long-term clinical improvement in MPTP-lesioned primates after gene therapy with AAV-hAADC. Mol Ther 2006;14:564–570. [PubMed: 16829205]
16. Forsayeth JR, Eberling JL, Sanftner LM, Zhen Z, Pivirotto P, Bringas J, et al. A dose-ranging study of AAV-hAADC therapy in Parkinsonian monkeys. Mol Ther 2006;14:571–577. [PubMed: 16781894]
17. Hadaczek P, Yamashita Y, Mirek H, Tamas L, Bohn MC, Noble C, et al. The “perivascular pump” driven by arterial pulsation is a powerful mechanism for the distribution of therapeutic molecules within the brain. Mol Ther 2006;14:69–78. [PubMed: 16650807]
18. Krauze MT, Saito R, Noble C, Bringas J, Forsayeth J, McKnight TR, et al. Effects of the perivascular space on convection-enhanced delivery of liposomes in primate putamen. Exp Neurol 2005;196:104–111. [PubMed: 16109410]
19. Hadaczek P, Mirek H, Bringas J, Cunningham J, Bankiewicz K. Basic fibroblast growth factor enhances transduction, distribution, and axonal transport of adeno-associated virus type 2 vector in rat brain. Hum Gene Ther 2004;15:469–479. [PubMed: 15144577]
20. Parent A, Smith Y. Differential dopaminergic innervation of the two pallidal segments in the squirrel monkey (*Saimiri sciureus*). Brain Res 1987;426:397–400. [PubMed: 2891410]
21. Smith Y, Lavoie B, Dumas J, Parent A. Evidence for a distinct nigropallidal dopaminergic projection in the squirrel monkey. Brain Res 1989;482:381–386. [PubMed: 2565144]
22. Moore RY. Organization of midbrain dopamine systems and the pathophysiology of Parkinson's disease. Parkinsonism Relat Disord 2003;9(suppl 2):S65–S71. [PubMed: 12915070]

23. Mounayar S, Boulet S, Tande D, Jan C, Pessiglione M, Hirsch EC, et al. A new model to study compensatory mechanisms in MPTP-treated monkeys exhibiting recovery. Brain 2007;130:2898–2914. [PubMed: 17855373]
24. Parent A, Lavoie B, Smith Y, Bedard P. The dopaminergic nigropallidal projection in primates: distinct cellular origin and relative sparing in MPTP-treated monkeys. Adv Neurol 1990;53:111–116. [PubMed: 1978512]
25. Whone AL, Moore RY, Piccini PP, Brooks DJ. Plasticity of the nigropallidal pathway in Parkinson's disease. Ann Neurol 2003;53:206–213. [PubMed: 12557287]
26. Piggott MA, Marshall EF, Thomas N, Lloyd S, Court JA, Jaros E, et al. Striatal dopaminergic markers in dementia with Lewy bodies, Alzheimer's and Parkinson's diseases: rostrocaudal distribution. Brain 1999;122:1449–1468. [PubMed: 10430831]
27. Yang M, Card JP, Tirabassi RS, Miselis RR, Enquist LW. Retrograde, transneuronal spread of pseudorabies virus in defined neuronal circuitry of the rat brain is facilitated by gE mutations that reduce virulence. J Virol 1999;73:4350–4359. [PubMed: 10196333]
28. Sun N, Cassell MD, Perlman S. Anterograde, transneuronal transport of herpes simplex virus type 1 strain H129 in the murine visual system. J Virol 1996;70:5405–5413. [PubMed: 8764051]
29. Saito R, Krauze MT, Bringas JR, Noble C, McKnight TR, Jackson P, et al. Gadolinium-loaded liposomes allow for real-time magnetic resonance imaging of convection-enhanced delivery in the primate brain. Exp Neurol 2005;196:381–389. [PubMed: 16197944]
30. Rennels ML, Gregory TF, Blaumanis OR, Fujimoto K, Grady PA. Evidence for a “paravascular” fluid circulation in the mammalian central nervous system, provided by the rapid distribution of tracer protein throughout the brain from the subarachnoid space. Brain Res 1985;326:47–63. [PubMed: 3971148]
31. Rennels ML, Blaumanis OR, Grady PA. Rapid solute transport throughout the brain via paravascular fluid pathways. Adv Neurol 1990;52:431–439. [PubMed: 2396537]
32. Donzelli R, Marinkovic S, Brigante L, de Divitiis O, Nikodijevic I, Schonauer C, et al. Territories of the perforating (lenticulostriate) branches of the middle cerebral artery. Surg Radiol Anat 1998;20:393–398. [PubMed: 9932322]
33. Russmann H, Vingerhoets F, Ghika J, Maeder P, Bogousslavsky J. Acute infarction limited to the lenticular nucleus: clinical, etiologic, and topographic features. Arch Neurol 2003;60:351–355. [PubMed: 12633146]
34. Wolfram-Gabel R, Maillot C. Vascular networks of the nucleus lentiformis. Surg Radiol Anat 1994;16:373–377. [PubMed: 7725192]
35. Varenika V, Dickenson P, Bringas J, LeCouteur R, Higgins R, Park J, et al. Realtime imaging of CED in the brain permits detection of infusate leakage. J Neurosurg. 2007in press
36. Burger C, Gorbatyuk OS, Velardo MJ, Peden CS, Williams P, Zolotukhin S, et al. Recombinant AAV viral vectors pseudotyped with viral capsids from serotypes 1, 2, and 5 display differential efficiency and cell tropism after delivery to different regions of the central nervous system. Mol Ther 2004;10:302–317. [PubMed: 15294177]
37. Paterna JC, Feldon J, Bueler H. Transduction profiles of recombinant adeno-associated virus vectors derived from serotypes 2 and 5 in the nigrostriatal system of rats. J Virol 2004;78:6808–6817. [PubMed: 15194756]
38. Cearley CN, Wolfe JH. Transduction characteristics of adeno-associated virus vectors expressing cap serotypes 7, 8, 9, and Rh10 in the mouse brain. Mol Ther 2006;13:528–537. [PubMed: 16413228]
39. Taymans JM, Vandenberghe LH, Haute CV, Thiry I, Deroose CM, Mortelmans L, et al. Comparative analysis of adeno-associated viral vector serotypes 1, 2, 5, 7, and 8 in mouse brain. Hum Gene Ther 2007;18:195–206. [PubMed: 17343566]
40. Gao G, Vandenberghe LH, Wilson JM. New recombinant serotypes of AAV vectors. Curr Gene Ther 2005;5:285–297. [PubMed: 15975006]
41. Chirmule N, Propert K, Magosin S, Qian Y, Qian R, Wilson J. Immune responses to adenovirus and adeno-associated virus in humans. Gene Ther 1999;6:1574–1583. [PubMed: 10490767]
42. Moskalenko M, Chen L, van Roey M, Donahue BA, Snyder RO, McArthur JG, et al. Epitope mapping of human anti-adeno-associated virus type 2 neutralizing antibodies: implications for gene therapy and virus structure. J Virol 2000;74:1761–1766. [PubMed: 10644347]

43. Erles K, Sebokova P, Schlehofer JR. Update on the prevalence of serum antibodies (IgG and IgM) to adeno-associated virus (AAV). J Med Virol 1999;59:406–411. [PubMed: 10502275]

44. Mastakov MY, Baer K, Symes CW, Leichtlein CB, Kotin RM, During MJ. Immunological aspects of recombinant adeno-associated virus delivery to the mammalian brain. J Virol 2002;76:8446–8454. [PubMed: 12134047]

45. Matsushita T, Elliger S, Elliger C, Podsakoff G, Villarreal L, Kurtzman GJ, et al. Adeno-associated virus vectors can be efficiently produced without helper virus. Gene Ther 1998;5:938–945. [PubMed: 9813665]

46. Wright JF, Qu G, Tang C, Sommer JM. Recombinant adeno-associated virus: formulation challenges and strategies for a gene therapy vector. Curr Opin Drug Discov Devel 2003;6:174–178.

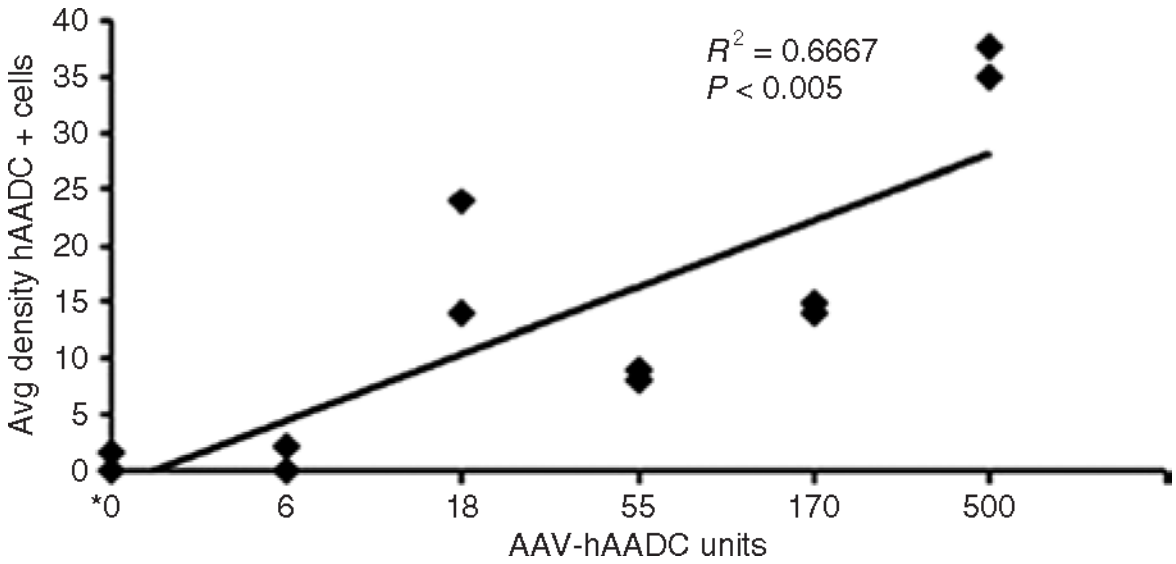

Figure 1. Average density of human aromatic L-amino acid decarboxylase (hAADC)-positive cells in putamen

The average density of distribution of hAADC-positive cells (mean cell count (±SD) per mm^2) that was detected by immunohistochemistry was estimated in the putamen for all animals, using National Institutes of Health Image software. The density of distribution was determined using a counting grid at six randomly selected sites in each section, and six sections (on average) were examined from each animal. Although AAV2-hAADC was infused into both hemispheres, only the side contralateral to 1-methyl-4-phenyl-1,2,3,6-tetrahydropyridine intracarotid artery administration was examined, because the ipsilateral side was processed for PCR and high-performance liquid chromatography analyses. The dose units are therefore represented as per hemisphere. *Control animals received 0 U AAV2-hAADC and 500 U AAV2-GFP. Avg, average; AAV2, adeno-associated virus type-2; GFP, green fluorescent protein.

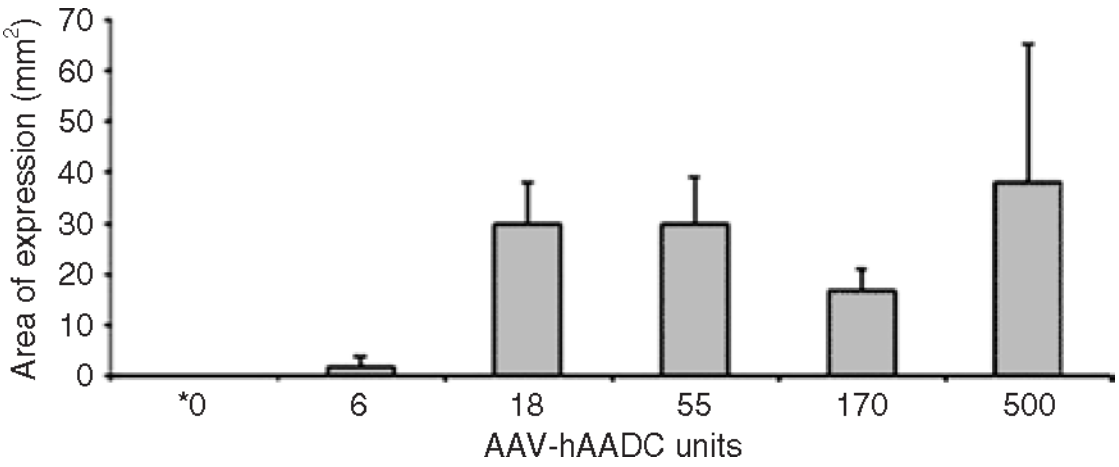

Figure 2. Average area of AAV2-hAADC expression in putamen

Area of human aromatic L-amino acid decarboxylase (hAADC) distribution within the putamen was determined on the side of the brain contralateral to 1-methyl-4-phenyl-1,2,3,6-tetrahydropyridine intracarotid artery administration. Random sections through the putamen were selected and the area (mean mm^2 ± SD) in which hAADC-positive cells were present was calculated using National Institutes of Health Image software. Six sections, on an average, were evaluated from each animal, and $n = 2$ animals/group. The dose units are represented as per hemisphere. *Control animals received 0 U AAV2-hAADC and 500 U AAV2-GFP. AAV2, adeno-associated virus type-2; GFP, green fluorescent protein.

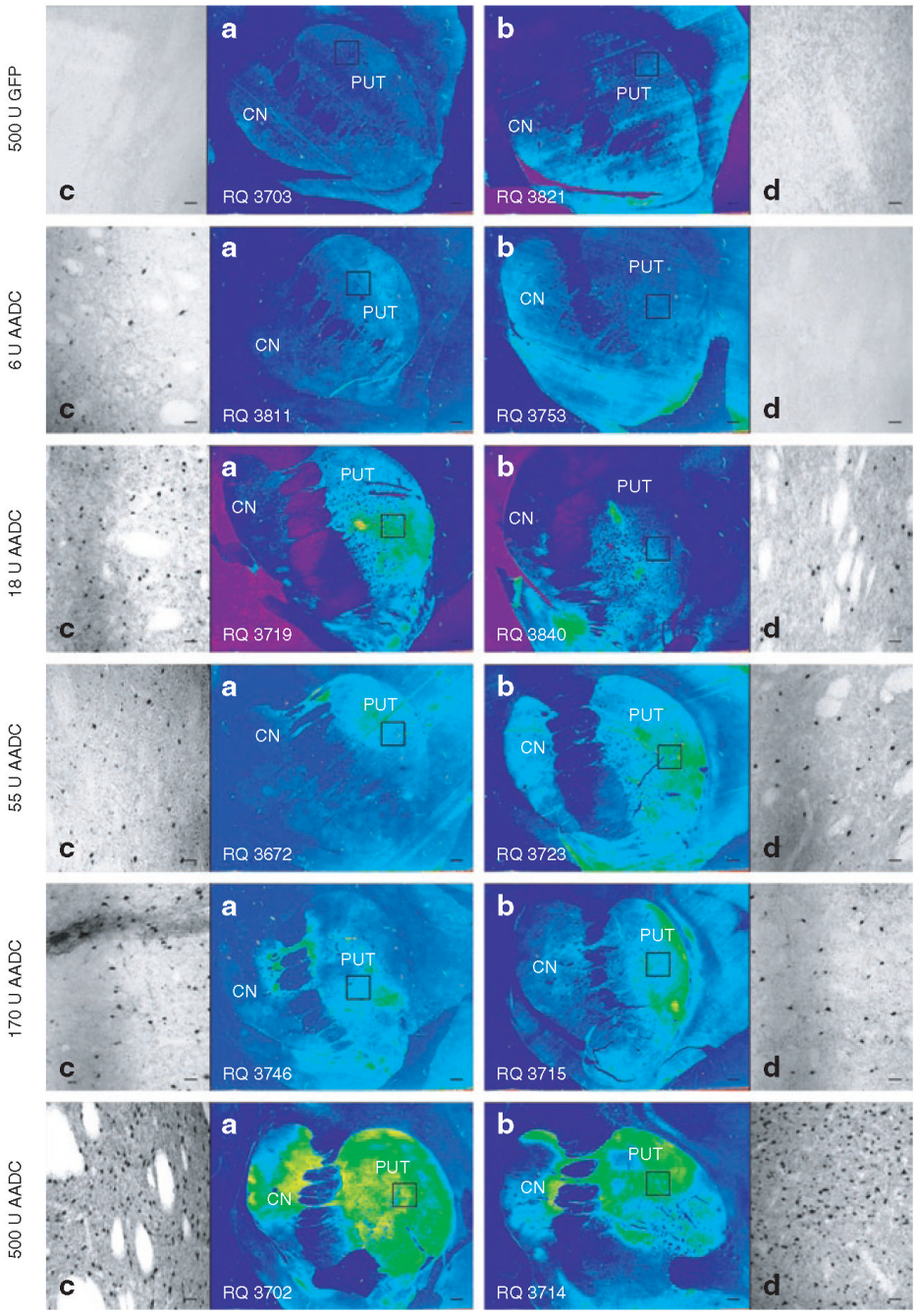

Figure 3. Immunohistochemical detection of AAV2-hAADC in escalating dose groups

Immunohistochemical staining of brain tissue from each dose group was performed with anti-hAADC primary antibodies followed by secondary antibodies labeled with immunoperoxidase. Images shown are (**a**,**b**) ×20 and (**c**,**d**) ×100 original magnification. Scale bars = 2 mm (**a**,**b**) and 100 μm (**c**,**d**). CN, caudate nucleus; GFP, green fluorescent protein; hAADC, human aromatic L-amino acid decarboxylase; PUT, putamen.

Table 1

Distribution of hAADC DNA in monkey brain tissues after AAV2 infusion into putamen

Animal	AAV2	Dose	OC	MC	CG	FC	PT[a]	CN[a]	GPi[a]	GPe [a]	TH	SNc[a]	SNr[a]	STN[a]	CB
Copies hAADC/μg monkey DNA															
RQ3714	hAADC	500	NEG	186 ± 53	2,766 ± 148	881[b] ± 981	1,218,084 ± 24,011	68,436 ± 2,475	24,250[c] ± 1,797	27,9187[c] ± 6,994	1,062 ± 617	63[b] ± 104	459[b] ± 382	82[b] ± 36	NEG[b]
RQ3702	hAADC	500	NEG	1,876 ± 151	933[b] ± 116	NEG	73,545 ± 1,918	NEG	13,704 ± 543	64,534 ± 1,996	64 ± 25	NS	NS	234[c] ± 16	NEG[b]
RQ3746	hAADC	170	NEG	5,500 ± 260	708 ± 65	NEG	142,533 ± 3,068	122 ± 29	NEG	NEG[c]	NEG	44[c] ± 13	NEG[c]	NEG[c]	NEG
RQ3715[d]	hAADC	17052 ± 21	880 ± 113	1,219[b] ± 184	407 ± 60	329 ± 47	681 ± 103	60[c] ± 11	NEG	100[c] ± 21	79[c] ± 9	NS	NEG[c]	NEG	
RQ3723	hAADC	55	NEG	NEG[b]	40 ± 11	NEG	56,598 ± 803	1,396[b] ± 131	89 ± 17	121 ± 24	NEG	NEG[c]	NEG[c]	77[b] ± 21	NEG
RQ3672	hAADC	55	NEG	363 ± 38	72 ± 20	NEG	36,205 ± 1,921	NEG	460 ± 79	46,759 ± 1,102	NEG[c]	NS	NS	NEG[c]	NEG
RQ3719	hAADC	18	NEG	NEG	NEG	NEG	92,345 ± 2,314	NEG	NEG	1,485 ± 151	NEG	NEG	NEG[c]	52[c] ± 11	NEG
RQ3840	hAADC	18	NEG	NEG	NEG	NEG	99,464 ± 4,326	NEG	151 ± 3	1,084 ± 79	NEG	NS	NS	NEG	NEG
RQ3811	hAADC	6	NEG	NEG	NEG	NEG	1,975 ± 213	NEG	NEG[b,c]	84[b] ± 17	NEG[c]	NEG[c]	NEG[c]	NEG[b]	NEG
RQ3753	hAADC	6	NEG	NEG	NEG	NEG	4,855 ± 228	NEG	5,271 ± 159	3,911[c] ± 142	NEG	NEG[c]	NEG[c]	NS	NEG
RQ3703	GFP	500	NEG	NEG	NEG	NEG	NEG	NEG	NEG[b,c]	NEG[c]	NEG[c]	NEG[c]	NEG[c]	NEG	NEG
RQ3821	GFP	500	NEG	NEG	NEG	NEG	NEG	NEG	NEG	NEG	NEG	NEG[c]	NEG	NEG	NEG
% Total copy number															
RQ3714	hAADC	500	0	<1%	<1%	<1%	76%	4%	2%	17%	<1%	<1%	<1%	<1%	0
RQ3702	hAADC	500	0	1%	<1%	0	47%	0	9%	42%	<1%	NS	NS	<1%	0
RQ3746	hAADC	170	0	4%	<1%	0	96%	<1%	0	0	0	0	0	0	0
RQ3715[d]	hAADC	170	1%	24%	33%	11%	9%	18%	0	0	3%	2%	NS	0	0
RQ3723	hAADC	55	0	0	<1%	0	97%	2%	<1%	<1%	0	0	0	<1%	0
RQ3672	hAADC	55	0	<1%	<1%	0	43%	0	<1%	56%	0	NS	NS	0	0
RQ3719	hAADC	18	0	0	0	0	98%	0	0	2%	0	0	0	<1%	0
RQ3840	hAADC	18	0	0	0	0	99%	0	0	1%	0	NS	NS	0	0
RQ3811	hAADC	6	0	0	0	0	96%	0	0	4%	0	0	0	0	0
RQ3753	hAADC	6	0	0	0	0	35%	0	37%	28%	0	0	0	NS	0
RQ3703	GFP	500	0	0	0	0	0	0	0	0	0	0	0	0	0
RQ3821	GFP	500	0	0	0	0	0	0	0	0	0	0	0	0	0

Abbreviations: AAV2, adeno-associated virus type-2; GFP, green fluorescent protein; NEG, below lower limit of quantitation (<40 copies hAADC/μg genomic DNA); NS, no sample collected; OC, occipital cortex; MC, temporal motor cortex; CG, cingulate gyrus; FC, frontal cortex; PT, Putamen; CN, caudate nucleus; GPi, globus pallidus internus; GPe, globus pallidus externus; TH, thalamus; SNc, substantia nigra compacta; SNr, substantia nigra reticulata; STN, subthalamic nucleus; CB, cerebellum.

Six months after vector infusion, PCR was used to quantitate human aromatic L-amino acid decarboxylase (hAADC) complementary DNA in 13 regions from the right side of the brain. Results shown are copy number hAADC (mean ± SD)/μg monkey DNA (top panel) and percentage each tissue contributed to the total PCR signal in any given animal brain (bottom panel).

[a] Basal ganglia tissue.

[b] PCR efficiency (as defined by % recovery of target DNA spiked into the reaction) was <75%.

[c] Results based on <2 μg of analyzed DNA.

[d] RQ3715 is an outlier.

Table 2

Neutralizing antibody response after AAV2 infusion into brain

Animal	AAV2	Dose	Baseline AAV2 neutralizing Ab titer	Post-AAV2 neutralizing Ab titer
RQ3714	hAADC	500	1:10–31	1:316–1,000
RQ3702	hAADC	500	1:10–31	1:31–100
RQ3746	hAADC	170	<1:10	1:316–1,000
RQ3715	hAADC	170	<1:10	<1:3
RQ3723	hAADC	55	1:10	1:3–10
RQ3672	hAADC	55	<1:10	1:10–30
RQ3719	hAADC	18	1:10–31	1:31–100
RQ3840	hAADC	18	1:10–31	1:31–100
RQ3811	hAADC	6	1:10–1:50	1:31–100
RQ3753	hAADC	6	<1:10	<1:3
RQ3703	GFP	500	<1:10	1:100–316
RQ3821	GFP	500	<1:10	1:316–1,000

Abbreviations: AAV2, adeno-associated virus type-2; GFP, green fluorescent protein; hAADC, human aromatic l-amino acid decarboxylase.

Serum samples from monkeys infused in the putamen with AAV2-hAADC or AAV2-GFP control were evaluated for development of neutralizing antibodies to AAV2 capsid protein. Dose is AAV2 units per hemisphere. Samples were collected at baseline (prior to AAV2 treatment) and 6 months postvector infusion.